

## Surface and Interfacial Structures of Silsesquioxane-terminated Polystyrene Thin Films

Kyota Miyamoto<sup>1</sup>, Nao Hosaka<sup>1</sup>, Motoyasu Kobayashi<sup>2</sup>,  
Hideyuki Otsuka<sup>1,2</sup>, Norifumi Yamada<sup>3</sup>, Naoya Torikai<sup>3</sup> and Atsushi Takahara<sup>1,2\*</sup>  
<sup>1</sup>Graduate School of Engineering, <sup>2</sup>Institute for Materials Chemistry and Engineering, Kyushu University  
Hakozaki, Higashi-ku, Fukuoka 812-8581, JAPAN, <sup>3</sup>KENS, Oho, Tsukuba, Ibaraki 305-0801, JAPAN  
Fax: 81-92-642-2715, e-mail: takahara@cstf.kyushu-u.ac.jp

Thermal stability of thin films composed of silsesquioxane-terminated polystyrene (PS-POSS), prepared by nitroxide-mediated radical polymerization of styrene with POSS-containing initiator having 2,2,6,6-tetramethylpiperidine-1-oxyl (TEMPO)-based alkoxyamine unit, was investigated. The introduction of POSS as PS end group can actually stabilize PS films against dewetting. Rheological measurement revealed that the polymer dynamics were profoundly affected by the presence of POSS end groups in low molecular weight region ( $M_n \approx 2000$ ), while those were nearly unaffected in high molecular weight region ( $M_n \approx 40000$ ). Neutron reflectivity measurement of deuterated PS-POSS thin films revealed that the POSS moiety of PS-POSS formed enrichment layer at the surface and interface of the film. The segregation of POSS, which changes the surface and interfacial free energy of the film, can be an important factor in the dewetting inhibition effect.

Key words: dewetting, silsesquioxane, neutron reflectivity

### 1. INTRODUCTION

Polymer thin films have numerous technological applications which require the presence of a homogeneous film. However, producing stable films is problematic since the polymer thin films tend to dewet from the substrates.<sup>1</sup> Various approaches have been adopted to stabilize these films against dewetting.<sup>2,3</sup>

Recently, much interest has focused on the use of functional additives to improve the thin film stability. Barnes et al. discovered that the addition of fullerene nanoparticles effectively stabilized the film against breakup.<sup>4</sup> Mackay et al. reported that dendrimer and polymer nanoparticles also behave similarly to the fullerene in inhibiting the dewetting of polymer thin films.<sup>5,6</sup>

Polyhedral oligomeric silsesquioxanes (POSS) have gained considerable attention due to their organic-inorganic hybrid structure which consists of a silica cage with organic groups. The salient feature of this nanosized building block is the ability to functionalize the silicon corners with a variety of organic substituents. POSS cages can be incorporated into polymer systems via polymerization, grafting, and blending by introducing the specific functionalities. By such hybridization, properties superior to the organic material alone are realized, offering exciting possibilities for the development of new materials.<sup>7-9</sup>

Our previous study showed that the blending of octacyclopentyl-POSS (CpPOSS) with the polystyrene (PS) thin films led to an inhibition of dewetting in the films.<sup>10</sup> Furthermore, the enhancement of the thermal stability of the PS thin films by the addition of POSS-terminated PS (PS-POSS), prepared to improve the affinity of POSS with PS, was also demonstrated.<sup>11</sup> The present work is focused on the thermal stability of PS-POSS thin films, whose surface and interfacial structures are investigated by the use of neutron

reflectivity technique. The effect of the POSS as the chain end group on the viscosity and the glass transition temperature ( $T_g$ ) of PS that might be associated with the dewetting inhibition effect is also examined.

### 2. EXPERIMENTAL

#### 2.1 Materials

4-Hydroxy-TEMPO<sup>12</sup> and 4-methoxy-TEMPO<sup>13</sup> were prepared and purified as previously reported. 1-[Isocyanatopropyl]dimethylsilyl-3,5,7,9,11,13,15-heptacyclopentylpentacyclo[9.5.1.1<sup>3,9</sup>.1<sup>5,15</sup>.1<sup>7,13</sup>]-octasiloxane (POSS-NCO) was purchased from Aldrich Chemical Co. Styrene (99+%) was obtained from Wako Pure Chemical Industries and purified by distillation under reduced pressure over calcium hydride. Polystyrene was purchased from Polymer Source, Inc. All other reagents were purchased from commercial sources and used as received. The silicon wafer substrates were purchased from Sumitomo Mitsubishi Silicon Co., and cleaned by immersion in the mixture of H<sub>2</sub>SO<sub>4</sub> (97%) and H<sub>2</sub>O<sub>2</sub> (34.5%) with volume ratio of 7:3 for 1 h at 353 K, rinsed in deionized water and dried under vacuum before spin-coating.

#### 2.2 Measurements

<sup>1</sup>H and <sup>13</sup>C NMR spectra were recorded on a JEOL JNM-EX400 spectrometer using tetramethylsilane (TMS) as an internal standard in chloroform-*d* (CDCl<sub>3</sub>). IR spectra were obtained with Perkin-Elmer Spectrum One infrared spectrometer. The number average molecular weight ( $M_n$ ) and molecular weight distribution (MWD) were estimated by gel permeation chromatographic (GPC) analysis. GPC was carried out at 40 °C on JASCO high performance liquid chromatography (HPLC) system equipped with a guard column (TOSOH TSKguardcolumn SuperH-L), three mixed columns (TOSOH TSKgel SuperH6000, 4000,

and 2500), and a differential refractometer. Tetrahydrofuran (THF) was used as the eluent at a flow rate of 0.6 mL/min. Polystyrene standards ( $M_n = 800$ – $152000$ ;  $M_w/M_n = 1.03$ – $1.10$ ) were used to calibrate the GPC system.

Differential scanning calorimetry (DSC) was performed on DSC8230 (Rigaku) under nitrogen atmosphere at a heating rate of 10 K/min. Thermogram of the second heating process were stored and analyzed.

The rheological properties of the polymers were measured with a Physica MCR 101 (Anton Paar GmbH). A parallel plate geometry with a diameter of 8 mm and a gap of 1 mm was used for all measurements. Samples were tested at temperatures between 383 and 423 K under nitrogen atmosphere with oscillation frequencies ranging from 100 to 0.1 rad/s and strain amplitude of 1%. After the rheological measurement,  $M_n$  and MWD of the samples were monitored by GPC again in order to check the stability and damage of the polymers.

Neutron reflectivity (NR) measurements were performed using an advanced reflectometer for interface and surface analysis (ARISA) on H5 beamline of Neutron Science Laboratory, High Energy Accelerator Research Organization.<sup>14</sup> The theoretical NR was calculated using Parratt32 (version 1.5 HMI Berlin), and evaluated against the experimental data.

### 2.3 Synthesis of POSS-containing initiator

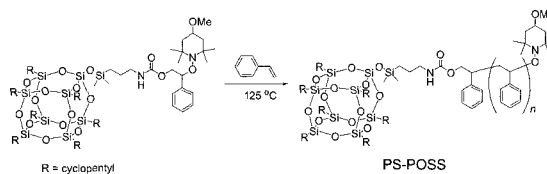
Catalytic amount of dibutyltin dilaurate was added to a dry toluene solution (3.5 mL) of the POSS-NCO (4.0 g, 3.8 mmol) and TEMPO-based alcohol (1.2 g, 3.8 mmol). The reaction mixture was stirred at room temperature under nitrogen for 24 h. The crude product was purified by flash chromatography using an eluent of ethyl acetate/hexane/chloroform (1/3/12, v/v/v) and dried under vacuum to give the POSS-containing initiator as a white powder (3.2 g, 62% yield). <sup>1</sup>H NMR:  $\delta$ /ppm 0.11 (s, 6H), 0.51 (m, 2H), 0.67 (s, 3H), 1.01 (m, 7H), 1.08 (s, 3H), 1.23 (s, 3H), 1.38 (s, 3H), 1.30–2.00 (m, 60H), 3.09 (m, 2H), 3.30 (s, 3H), 3.40 (m, 1H), 4.20 (dd,  $J = 6$  Hz, 11 Hz, 1H), 4.56 (m, 1H), 4.63 (dd,  $J = 6$  Hz, 11 Hz, 1H), 4.88 (t,  $J = 6$  Hz, 1H), 7.20–7.40 (m, aromatic). FT-IR (KBr,  $\text{cm}^{-1}$ ): 3100–2810, 1728 (C=O), 1522, 1452, 1252, 1200–1000, 913, 838, 757, 698, 505. Mass spectrum (FAB) 1365.

### 2.4 Polymerization

A mixture of the POSS-containing initiator (700 mg, 0.51 mmol) and styrene (1.5 mL, 13.1 mmol) was charged in a polymerization tube, degassed, and sealed off under vacuum. The mixture was incubated at 125 °C for 24 h, and after dilution with chloroform the solution was poured into methanol. The precipitate was further purified by reprecipitation with a chloroform/methanol system and dried under vacuum to give the PS-POSS as a white powder (1.3 g, 63% yield).  $M_n = 2500$ ,  $M_w/M_n = 1.11$ . <sup>1</sup>H NMR:  $\delta$ /ppm 0.01–0.60 (br), 0.80–2.60 (br, aliphatic H), 3.03 (br), 3.2–4.5 (br), 6.20–7.40 (br, aromatic H). FT-IR (NaCl,  $\text{cm}^{-1}$ ): 3100–2810, 1728 (C=O), 1602 (C=C), 1493, 1453, 1252, 1200–1000, 908, 838, 757, 698, 505.

### 2.5 Thin film preparation

Thin films were prepared by spin-coating the



**Scheme 1** Synthesis of well-defined PS-POSS by nitroxide-mediated radical polymerization.

polymers dissolved in toluene, which had been passed through a PTFE filter (pore size = 0.20  $\mu\text{m}$ ), onto acid-cleaned silicon wafers at 2000 rpm for 30 s. The concentration of the polymer solution was 3 wt %. Under these conditions the films produced were approximately 110 nm thick as determined by ellipsometry using Imaging Ellipsometer (Moritex Corp.). Spin-coated films were annealed under vacuum at 393 K for 3 h and quenched to room temperature. Reflective optical images were obtained with an optical microscope, OLYMPAS BX51 (Olympas Optical Co., Ltd.).

## 3. RESULTS AND DISCUSSION

### 3.1 Synthesis of silsesquioxane-terminated polystyrene

The synthesis of POSS-containing initiator was carried out by the addition reaction of POSS with an isocyanate pendant group to the TEMPO-based alkoxyamine with a hydroxy group. PS-POSS were prepared by nitroxide-mediated radical polymerization (NMRP)<sup>15</sup> using this initiator (Scheme 1). <sup>1</sup>H NMR detected a weak proton signal at 4.56 ppm attributed to the urethane linking groups, while a proton signal of the  $-\text{CH}_2-\text{NCO}$  group at 3.27 ppm was disappeared. The structure of the initiator and PS-POSS was also confirmed by comparison of the Fourier transform infrared spectra of the two starting materials and the final product. After the addition reaction, the isocyanate absorption band at 2270  $\text{cm}^{-1}$  of the starting material disappeared and the absorption corresponding to the stretching vibration of urethane carbonyl groups was observed at 1728  $\text{cm}^{-1}$ . The synthesized PS-POSS showed the characteristic PS absorbance. These results concluded that the PS having a POSS at the chain end was successfully obtained.

### 3.2 Thermal stability of PS-POSS thin films

Optical micrographs of (a) 110-nm thick PS2.1k ( $M_n = 2100$ ,  $M_w/M_n = 1.06$ ) and (b) 113-nm thick PS-POSS2.5k ( $M_n = 2500$ ,  $M_w/M_n = 1.11$ ) thin films, after annealing, are shown in Fig. 1. The bare substrate was observed as a consequence of the complete dewetting of PS2.1k film, in contrast, no appreciable dewetting was observed in the PS-POSS2.5k film. This suggests that the introduction of POSS as PS end group can inhibit the dewetting of the film. Interestingly, similar results are obtained for the PS-POSS43k film, which contained less POSS fraction compared to the PS-POSS2.5k. Fig. 2 shows the optical micrographs of (a) 113-nm thick PS44k ( $M_n = 44000$ ,  $M_w/M_n = 1.04$ ) and (b) 114-nm thick PS-POSS43k ( $M_n = 43000$ ,  $M_w/M_n = 1.11$ ) thin films annealed at 393 K for 96 h. The pure PS44k film broke up by the creation of holes, whereas PS-POSS43k film did not dewet at all.

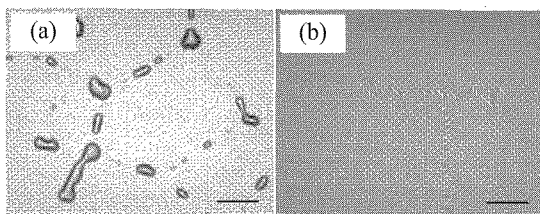


**Fig. 1** Optical micrographs of (a) PS2.1k and (b) PS-POSS2.5k films annealed at 393 K for 3 h. The length of the bar is 100  $\mu\text{m}$ .

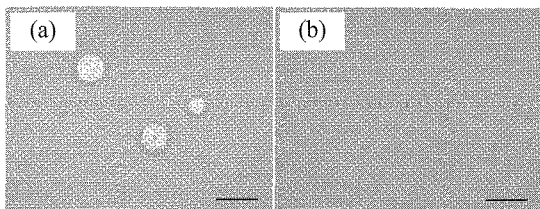


**Fig. 2** Optical micrographs of (a) PS44k and (b) PS-POSS43k films annealed at 393 K for 96 h. The length of the bar is 100  $\mu\text{m}$ .

### 3.3 Rheological characterization of PS-POSS

To evaluate the effect of the bulk viscoelastic properties of PS-POSS to the dewetting inhibition, the rheological measurements were carried out. It is expected that the introduction of the POSS moiety into the end group of polymer chains affects the physical properties of the polymer dramatically. Rheological characterization is important for comparing the viscoelastic behavior of the PS and PS-POSS systems. Fig. 3 illustrates the master curves of the storage modulus  $G'$  for PS2.1k and PS-POSS2.5k. The master curves, generated by applying the principle of time-temperature superposition to isothermal frequency scans, were shifted to a reference temperature ( $T_0 = 383$  K). The pure PS2.1k behaves as a Newtonian liquid with the viscoelastic properties exhibiting liquidlike characteristics, while PS-POSS2.5k exhibits pseudo-solid-like behavior. The low frequency slope of PS-POSS2.5k is approximately 0 in comparison to a typical slope of 2 for a Newtonian liquid. It was not possible to attain the terminal regime for the PS-POSS2.5k within the range of temperatures investigated and under the current experimental conditions. It is likely that the rheological behavior of

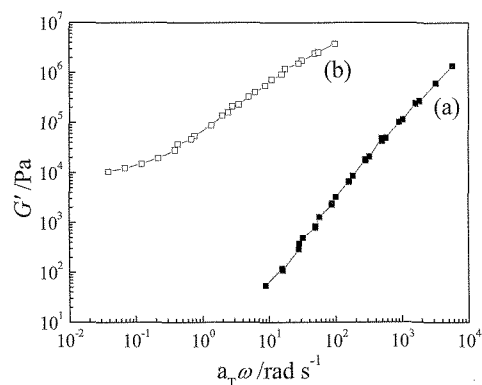


**Fig. 3**  $G'$  master curves of (a) PS2.1k and (b) PS-POSS2.5k at reference temperature of 383 K.

**Table I** Zero-shear-rate viscosities  $\eta_0$  and  $T_g$  values of PS2.1k and PS-POSS2.5k.

polymer	$\eta_0$ /Pa·s ( $T_0=383$ K)	$T_g$ /K
PS2.1k	$3.02 \times 10^2$	340
PS-POSS2.5k	$7.81 \times 10^5$	348

**Table II** Zero-shear-rate viscosities  $\eta_0$  and  $T_g$  values of PS44k and PS-POSS43k.

polymer	$\eta_0$ /Pa·s ( $T_0=413$ K)	$T_g$ /K
PS44k	$6.74 \times 10^4$	375
PS-POSS43k	$7.25 \times 10^4$	375

PS-POSS2.5k is strongly influenced by the presence of POSS end groups. This may lead to dramatically altered diffusion of PS chains. As mentioned before, after rheological characterization the samples were redissolved and the  $M_n$  and MWD were confirmed to be intact by GPC.

Zero-shear-rate viscosities,  $\eta_0$ , were calculated from the relation

$$\eta_0 = \lim_{\omega \rightarrow 0} \frac{G''}{\omega}$$

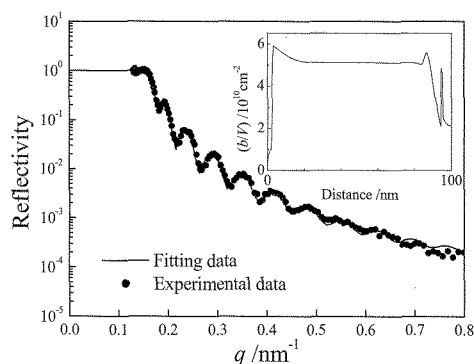
and were reported in Table I, with the  $T_g$  values obtained from DSC. The  $\eta_0$  and  $T_g$  of PS-POSS2.5k were higher than those of the pure PS2.1k, indicating that the massive POSS inorganic end groups strongly restricted the PS chain motion. The dewetting of a polymer film from a substrate has been observed to proceed with a velocity that is inversely proportional to the bulk viscosity of the dewetting fluid.<sup>16</sup> It was assumed that the increase of the viscosity resulted in the inhibition of film dewetting.

Table II summarized the  $\eta_0$  and  $T_g$  values of PS44k and PS-POSS43k. Comparison of Table I and Table II shows the influence of chain length on the rheology of the PS-POSS. There was no noticeable difference in the  $\eta_0$  and  $T_g$  values of PS44k and PS-POSS43k because of the decrease in the relative weight fraction of POSS moiety to PS by the increase of PS chain length. However, PS-POSS43k also gave rise to dewetting inhibition, as shown in Fig. 2, suggesting that some other factors attributing the film stabilization effect exist.

### 3.4 Neutron reflectivity of dPS-POSS

NR measurement was applied to examine the depth composition profile of the deuterated PS-POSS (dPS-POSS) thin film. dPS-POSS was prepared by NMRP of deuterated styrene using POSS-containing initiator, as the same procedure of PS-POSS. The intensity of the reflected neutron beam was recorded as a function of the scattering vector ( $q = 4\pi \sin \theta / \lambda$ ). Fig. 4 shows the reflectivity profile of dPS-POSS8.2k ( $M_n = 8200$ ,  $M_w/M_n = 1.07$ ) thin film. The solid line is the fit of the reflectivity profile and inset shows the neutron scattering length density ( $b/V$ ) profile used to generate the fit. The horizontal axis of the inset corresponds to the distance perpendicular to the film. Since  $b/V$  of the dPS is much larger than that of the POSS moiety, the dispersion state of the POSS moiety in the film can be detected.

The data were fit with a seven-layer model, which were POSS enrichment layer–dPS layer–bulk layer–dPS



**Fig. 4** NR data from dPS-POSS8.2k thin film annealed at 393 K for 2 h. The inset shows the scattering length density ( $b/V$ ) profile used to calculate the reflectivity profile as the solid line.

layer-POSS enrichment layer-silicon oxide-silicon. The first layer is the film surface with lower  $b/V$  than that of the third bulk layer because of the segregation of the POSS moiety of dPS-POSS. The second and fourth thin layers with high  $b/V$  between POSS enriched layers and the bulk region was due to the localization of dPS chains connected to the POSS end groups. At the fifth layer, substrate interface, it can be seen that the POSS moiety is located as well as the film surface. In the CpPOSS/PS blend thin films, similar enrichment of CpPOSS at the surface and interface was also observed.<sup>17</sup> The segregation of CpPOSS moiety to the substrate interface is analogous to the substrate coverage by several nanofillers.<sup>4,6</sup> The exact mechanism of the obtained dewetting inhibition effect was elusive, but it can be attributed to the change of the energetics of the surface and interface by the segregation of the POSS moiety.

#### 4. CONCLUSIONS

In summary, thermal stability of thin films composed of silsesquioxane-terminated polystyrene (PS-POSS), prepared by nitroxide-mediated radical polymerization of styrene with POSS-containing initiator having 2,2,6,6-tetramethylpiperidine-1-oxyl (TEMPO)-based alkoxyamine unit, was investigated. The introduction of POSS as a PS end group can actually stabilize PS films against dewetting. Rheological characterization showed that the polymer dynamics of PS-POSS2.5k ( $M_n = 2500$ ,  $M_w/M_n = 1.11$ ) were profoundly affected by the presence of POSS end group when compared with PS2.1k homopolymer ( $M_n = 2100$ ,  $M_w/M_n = 1.06$ ), while those of PS-POSS43k ( $M_n = 43000$ ,  $M_w/M_n = 1.11$ ) were nearly unaffected compared with PS44k ( $M_n = 44000$ ,  $M_w/M_n = 1.04$ ). Neutron reflectivity measurements revealed that the POSS moiety of PS-POSS formed enrichment layer at the surface and interface of the film. The segregation of POSS, which changes the surface and interfacial free energy of the film, can be an important factor in the dewetting inhibition effect.

#### ACKNOWLEDGMENTS

The present work was partially supported by a Grant-in-Aid for the 21st Century COE Program "Functional Innovation of Molecular Informatics" from the Ministry of Education, Culture, Sports, Science and Technology of Japan. N.H. acknowledges the financial support of Grant-in-Aid for JSPS Fellows.

#### References:

- [1] G. Reiter, *Langmuir*, **9**, 1344-1351 (1993).
- [2] R. Yerushalmi-Rozen, J. Klein, L. J. Fetters, *Science*, **263**, 793-795 (1994).
- [3] C. Yuan, M. Ouyang, J. T. Koberstein, *Macromolecules*, **32**, 2329-2333 (1999).
- [4] K. A. Barnes, A. Karim, J. F. Douglas, A. I. Nakatani, H. Gruell, E. J. Amis, *Macromolecules*, **33**, 4177-4185 (2000).
- [5] M. E. Mackay, Y. Hong, M. Jeong, S. Hong, T. P. Russell, C. J. Hawker, R. Vestberg, J. F. Douglas, *Langmuir*, **18**, 1877-1882 (2002).
- [6] R. S. Krishnan, M. E. Mackay, C. J. Hawker, B. Van Horn, *Langmuir*, **21**, 5770-5776 (2005).
- [7] T. S. Haddad, J. D. Lichtenhan, *Macromolecules*, **29**, 7302-7304 (1996).
- [8] K. M. Kim, D. K. Keum, Y. Chujo, *Macromolecules*, **36**, 867-875 (2003).
- [9] K. Koh, S. Sugiyama, T. Morinaga, K. Ohno, Y. Tsujii, T. Fukuda, M. Yamahiro, T. Iijima, H. Oikawa, K. Watanabe, T. Miyashita, *Macromolecules*, **38**, 1264-1270 (2005).
- [10] N. Hosaka, K. Tanaka, H. Otsuka, A. Takahara, *Compos. Interfaces*, **11**, 297-306 (2004).
- [11] K. Miyamoto, N. Hosaka, H. Otsuka, A. Takahara, *Chem. Lett.*, **35**, 1098-1099 (2006).
- [12] T. Kurosaki, K. W. Lee, M. Okawara, *J. Polym. Sci., Polym. Chem.*, **10**, 3295-3310 (1972).
- [13] T. Miyazawa, T. Endo, S. Shiihashi, M. Okawara, *J. Org. Chem.*, **50**, 1332-1334 (1985).
- [14] N. Torikai, M. Furusaka, H. Matsuoka, Y. Matsushita, M. Shibayama, A. Takahara, M. Takeda, S. Tasaki, H. Yamaoka, *Appl. Phys. A*, **74**(Suppl.), S264-S266 (2002).
- [15] C. J. Hawker, A. W. Bosman, E. Harth, *Chem. Review*, **101**, 3661-3688 (2001).
- [16] C. Redon, F. Brochard-Wyart, F. Rondelez, *Phys. Rev. Lett.*, **66**, 715-718 (1991).
- [17] N. Hosaka, N. Torikai, H. Otsuka, A. Takahara, *Langmuir*, **23**, 902-907 (2007).

(Received December 9, 2006; Accepted February 12, 2007)